# A NUMERICAL INVESTIGATION OF BLOOD FLOW THROUGH THE AORTIC VALVE

**Truong Sang Ha[1,*], Trung Dinh Nguyen[1], Van Chien Vu[1], Manh Hung Nguyen[1], Duc Quyen Vu[1], Manh Duc Nguyen[1]**

[1]*Faculty of Mechanical Engineering, Le Quy Don Technical University, Hanoi, Vietnam*

**Abstract**

This article aims to present a numerical analysis of blood flow in the aortic valve using fluid-structure interaction simulation. The finite element method is employed both for fluid and solid domains, and the monolithic scheme is used for the strong fluid-structure interaction coupling to solve well the two challenges: add-mass and large deformation problems. The Navier-Stokes equations are solved using the integrated method based on the unstructured grid on Arbitrary Lagrangian-Eulerian (ALE) framework with the total Lagrangian formulation is used for the non-linear behavior of the aortic valve. A smoothing technique based on the Laplace equation is employed to improve the mesh quality for both 2D and 3D geometries. The fluid characteristics, such as the velocity and pressure in the valve, are evaluated and analyzed in detail. The results show that velocity and pressure reach their maximum values when the valve is at its maximum opening. On the other hand, more vortices appear behind the valve during the closing phases. The simulation results can be used to help fully to predict and treat cardiovascular diseases.

***Keywords:*** *Blood flow; aortic valve; fluid-structure interaction; FEM; ALE.*

## 1. Introduction

Nowadays, aortic valve diseases are among the most common cardiovascular defects. Therefore, transcatheter aortic valve implantation (TAVI) has been carried out as an alternative for patients with severe aortic stenosis who are at high risk for surgical therapy. The biomechanical environment of TAVI is closely related to the interaction of the motion of the aorta and leaflets with blood flow. Therefore, fluid-structure interaction (FSI) simulation and an accurate blood prediction are essential for predicting and treating cardiovascular diseases. However, FSI simulation of a blood flow interacting with an aortic valve remains a big challenging problem.

B. Su et al. [1] studied the intraventricular flow in a patient-specific left ventricle in two-dimensional space (2D) integrated with mitral and aortic valves. Ventricular wall deformation was predefined based on MRI data while leaflet dynamics were predicted

[*] Email: sanght.st@lqdtu.edu.vn
https://doi.org/10.56651/lqdtu.jst.v17.n05.527

numerically by FSI. They have found that the 2D approach can qualitatively predict the intraventricular flow. An FSI modelling methodology for aortic valve hemodynamics using the commercial modelling software ANSYS was employed in [2]. The authors simulated the problem using fluid flow solver FLUENT and structural solver MECHANICAL APDL under ANSYS and coupled the solutions using System Coupling Module to enable FSI. Based on that, the influence of leaflet calcification on hemodynamic stresses and flow patterns was investigated. A study of the aortic valve motion was also reported in [3] that used an immersed boundary method to avoid the mesh deformed in the fluid domain. The blood flow through the aortic and heart valve was researched using the FSI algorithm in 2D and 3D space [4, 5]. We can see that the FSI approach is a widespread and robust tool to study the dynamic parameter of blood flow in a valve.

Although many publications on the aortic blood flow through the aortic valve, the problem has still been challenged and more research is needed. Because the fluid density is close to that of solid in the aortic artery/valve, the add-mass effect is strong and plays an important role in the numerical method. Moreover, due to the large deformation, the grid of fluid part is big distorted. These challenging problems are now open issues for numerical research. This article presents a numerical analysis of blood flow in an aortic valve using fluid-structure interaction simulation. The ALE framework with an unstructured grid in 2D/3D space using the finite element method for both fluid and solid domains is employed for the present numerical method.

## 2. Numerical method

### *2.1. Equations for incompressible blood flow*

The fluid domain is denoted by $\Omega^f$ with the boundary $\Gamma^f$. The incompressible Navier-Stokes equations can be written in the arbitrary Lagrangian-Eulerian form as follows [6, 7]:

$$\nabla \cdot \mathbf{v} = 0 \quad \text{in } \Omega^f, \tag{1a}$$

$$\rho^f \left[ \frac{\partial \mathbf{v}}{\partial t} + (\mathbf{v} - \mathbf{v}^m) \cdot \nabla \mathbf{v} \right] = -\nabla p + \nabla \cdot [\mu(\nabla \mathbf{v} + (\nabla \mathbf{v})^{\mathrm{T}})] \text{ in } \Omega^f \tag{1b}$$

where $\rho^f$, $\mathbf{v}$, $\mathbf{v}^m$, $\mu$ and $p$ denote the fluid density, the fluid velocity, the grid velocity, the dynamic fluid viscosity, and the pressure of fluid, respectively. The Dirichlet (Eq. 2a) and Neumann (Eq. 2b) boundary conditions are described as follows:

$$\mathbf{v} = \bar{\mathbf{v}} \quad \text{on } \Gamma_{\mathbf{v}}^{f}, \tag{2a}$$

$$\boldsymbol{\sigma}^{f} \cdot \mathbf{n}^{f} = \bar{\mathbf{t}}^{f} \quad \text{on } \Gamma_{\mathbf{t}}^{f} \tag{2b}$$

where $\mathbf{n}^f$ is the outer unit normal vector of the fluid boundary, $\boldsymbol{\sigma}^f$ is the fluid stress tensor, and $\Gamma_{\mathbf{v}}^{f}$ and $\Gamma_{\mathbf{t}}^{f}$ are the boundaries on which the velocity ($\bar{\mathbf{v}}$) and traction ($\bar{\mathbf{t}}^{f}$) are defined, respectively. The equations (1a), (1b) with conditions (2a), (2b) is the governing equation for fluid dynamics. Solving this equation to obtain the velocity and pressure field by the finite element method (FEM) is described in the later sections.

### *2.2. Equation for elastic solid of the aortic valve*

The solid domain is denoted by $\Omega^s$ with the boundary $\Gamma^s$. The deformation of the valve in the Lagrangian form is written by:

$$\rho^{s} \frac{\partial^{2}\mathbf{u}}{\partial t^{2}} = \nabla \cdot \boldsymbol{\sigma}^{s} \text{ in } \Omega^{s} \tag{3}$$

with boundary conditions:

$$\mathbf{u} = \bar{\mathbf{u}} \quad \text{on } \Gamma_{\mathbf{u}}^{s}, \tag{4a}$$

$$\boldsymbol{\sigma}^{s} \cdot \mathbf{n}^{s} = \bar{\mathbf{t}}^{s} \quad \text{on } \Gamma_{\mathbf{t}}^{s} \tag{4b}$$

where $\rho^s$, $\mathbf{u}$, and $\sigma^s$ denote the solid density, the displacement of structure, and the solid stress tensor, respectively. The constitutive equations of the solid domain in large deformation are written as [8]:

$$\boldsymbol{\sigma}^{s} = J^{-1}\mathbf{F}\mathbf{S}\mathbf{F}^{T}; \quad \mathbf{T} = \mathbf{S}\mathbf{F}^{T}; \quad \mathbf{S} = \mathbb{C} : \mathbf{E} \tag{5}$$

where $\mathbb{C}$ is the fourth-order tensor related to stiffness of material; $\mathbf{E}$ is the Green strain tensor; $\mathbf{T}$ and $\mathbf{S}$ are the first and second Piola-Kirchhoff stress tensors, respectively; and $\mathbf{F}$ and $J$ are the deformation gradient tensor and its Jacobian.

The Green strain tensor $\mathbf{E}$ is determined nonlinear with deformation by the following expression:

$$\mathbf{E} = \frac{1}{2}\left(\mathbf{C} - \mathbf{I}\right) = \frac{1}{2}\left[\left(\nabla_{\mathrm{X}}\mathbf{u}\right)^{\mathrm{T}} + \nabla_{\mathrm{X}}\mathbf{u} + \left(\nabla_{\mathrm{X}}\mathbf{u}\right)^{\mathrm{T}} \cdot \nabla_{\mathrm{X}}\mathbf{u}\right] \tag{6}$$

where $\mathbf{C}$ is the right Cauchy deformation tensor.

The deformation gradient tensor $\mathbf{F}$ and its Jacobian $J$ are given as follows: determined by the following expressions:

$$\mathbf{F} = \mathbf{I} + \nabla_{\mathrm{X}}\mathbf{u}; \quad J = \det(\mathbf{F}) \tag{7}$$

For a simple case, the Saint Venant-Kirchhoff model is usually used, and $\mathbb{C}$ is expressed by:

$$\mathbb{C} = \lambda(\mathbf{I} \otimes \mathbf{I}) + 2\eta\boldsymbol{\Pi} \tag{8}$$

where $\lambda$ and $\eta$ are the Lamé constants, and $\boldsymbol{\Pi}$ is the fourth-order unit tensor.

The Lamé constants $\lambda$ and $\eta$ can be computed from Young's modulus $E$ and Poison ratio $v$ as follows:

$$\lambda = \frac{\nu E}{(1+\nu)(1-2\nu)}; \quad \eta = \frac{E}{2(1+\nu)} \tag{9}$$

The fourth-order unit tensor $\boldsymbol{\Pi}$ is calculated by:

$$\boldsymbol{\Pi}_{ijkl} = \frac{1}{2}\left(\delta_{ik}\delta_{jl} + \delta_{il}\delta_{jk}\right) \tag{10}$$

where $\delta$ denotes the Dirac delta function.

### *2.3. FSI equation for strong coupling*

Let denote the interface between the fluid domain and solid domain (FS interface) by $\Gamma^{fs}$, $\Gamma^{fs} = \Gamma^f \cap \Gamma^s$. In the implicit coupling method, the velocity and traction need to satisfy the balance conditions. When a no-slip condition is applied, the velocity of the fluid is similar to that of solid on $\Gamma^{fs}$, and the balance condition can be written as follows:

$$\mathbf{v} = \frac{\partial \mathbf{u}}{\partial t} \quad \text{on } \Gamma^{fs} \tag{11}$$

Due to the force equilibrium condition, the traction should also be continued along the FS interface:

$$\boldsymbol{\sigma}^f \cdot \mathbf{n}^f + \boldsymbol{\sigma}^s \cdot \mathbf{n}^s = 0 \text{ on } \Gamma^{fs} \tag{12}$$

The direction of the unit normal vector of solid $\mathbf{n}^s$ is opposite to that of fluid $\mathbf{n}^f$ when the grids of fluid and solid domain along the FS interface are conformed.

For the simulation of large deformation, the strong coupling [7, 9] by using a monolithic approach is used to improve the convergence of the FSI problem. When the deformation is large, a smoothing technique based on the Laplace equation is employed to avoid the bad quality of the fluid mesh. The Total Lagrangian method is applied for nonlinear problems arising from the large deformation of the solid. The detailed expression of the FSI method is available in [9]. The obtained linear system can be solved by multigrid method to reduce the simulation time [10]. It should be noted that the present method using strong coupling and smoothing techniques has successfully treated the problems of the add-mass issue arising from the similarity of the density of fluid and solid as well as the large deformation problem of the solid wall.

## 3. Results and discussions

### *3.1. Validation code*

A pulsatile flow in a 2D circular channel with an elastic wall [9, 11] is considered to validate the accuracy of the code. Fig. 1 shows the schematics and boundary conditions of the pulsatile flow in a circular channel. A rigid body is set at the inside of the circular channel, and the curved elastic wall is fixed at the two ends. Pressure at the outlet is set to zero, and a parabolic profile of velocity is set at the inlet. The mean velocity $v_0$ is changed over time as follows:

$$v_0(t) = v_{max}\left(1-\cos(\pi t)\right) \tag{13}$$

Table 1 shows the dimension and physical property of the material for this benchmark problem. A grid independent test is performed with three grid resolutions employed, and the movement of point M in a short time is shown in Fig. 2. From the results, the medium grid with the number of nodes for fluid and solid domains are 4,961 and 1,089 as shown in Fig. 3 is used. It is noted that the quadratic element with 6 nodes is used for vector variables (displacement and velocity), and a linear element is adopted for the pressure of fluid (P2P1 element). The flow is simulated for 3.6 seconds with time step $\Delta t = 2.0 \times 10^{-3}\text{s}$. The solid wall is largely deformed under the traction of fluid flow into a soft wall. Fig. 4 illustrates the revolution of deformation of point M. The results agree well with the proposed literature [9, 11]. Fig. 5 demonstrates the velocity field together with the deformation of the channel wall at different instant times.

*Table 1. Dimension of the simulation geometry*

| Dimension | Symbol | Value |
|---|---|---|
| Width of circular channel | $H$ | 0.02 m |
| Thickness of circular channel | $T$ | 0.005 m |
| Radius of rigid body | $R$ | 0.02 m |
| Fluid density | $\rho^f$ | 1.18 kg/m$^3$ |
| Dynamic fluid viscosity | $\mu$ | $14.3 \times 10^{-4}$ N·s/m$^2$ |
| Density of solid | $\rho^s$ | $1.13 \times 10^2$ kg/m$^3$ |
| Young's modulus | $E$ | $2.0 \times 10^4$ Pa |
| Poisson ratio | $v$ | 0.4 |
| Maximum velocity at the inlet | $v_{max}$ | 0.2 m/s |

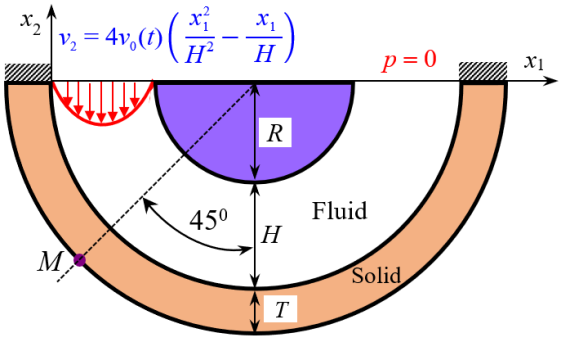


*Fig. 1. Schematic of the flow in a circular channel [9].*

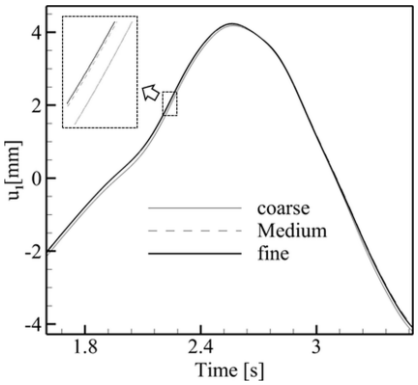


*Fig. 2. Grid independent test.*

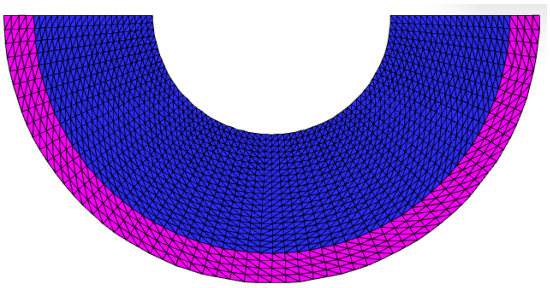

*Fig. 3. Grids fluid and solid used for simulation.*

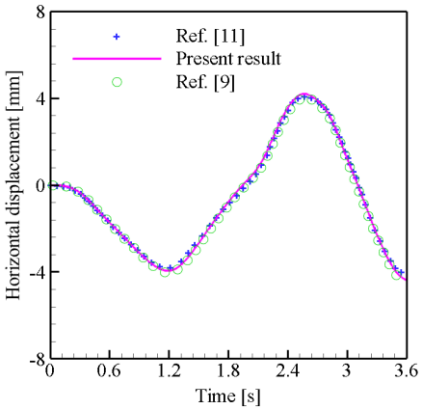


*Fig. 4. Revolution of deformation of point M.*

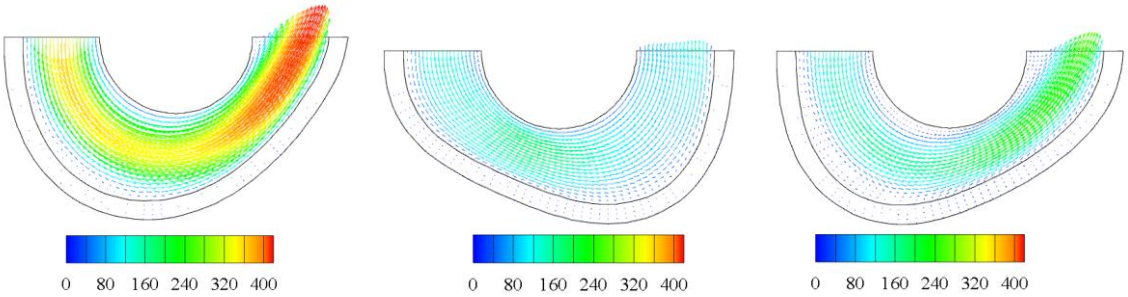


*a) Time = 1.2 s* *b) Time = 2.4 s* *c) Time = 3.6 s*

*Fig. 5. Velocity field at different instant time [cm/s].*

### *3.2. Blood flow through 2D aortic valve*

The proposed code validated in section 3.1 has been applied to simulate the blood flow through an aortic valve. Based on geometries of the aortic valve in [3, 4], we have created a simple aortic valve in 2D space, as shown in Fig. 6. The width of $D$ is set by 0.02 m and the length of $L$ = 0.022 m, the fluid is incompressible with the density of $\rho^f = 10^3$ kg/m$^3$ and dynamic viscosity of $\mu = 4 \times 10^{-3}$ Ns/m$^2$ as the property of human

blood. For the aortic valve domain, the linear elastic described by Saint - Kirchhof model with Young's modulus of $E = 1 \times 10^5$ Pa and the Poisson ratio of $v = 0.4$ is employed. A zero pressure is set at the outlet, and a full development blood flow at the inlet with the mean velocity $v(t)$ is changed over time as follows:

$$v(t) = v_{max} \sin(\pi t) \tag{14}$$

where $v_{max} = 0.1$ m/s.

After the grid-dependent test, the grid shown in Fig. 7 is used for this simulation since it is enough to get accurate results. The grid includes 9,910 nodes and 4,847 elements (4,767 for fluid and 80 for solid domain), and a higher resolution is placed around the valve. The time step is set to $\Delta t = 1.0 \times 10^{-3}$ s, and the simulation is handled for 2.2 seconds.

The velocity field and pressure contours are demonstrated in Fig. 8 for different time instants. In the systolic phase, the blood enters to the valve (time $t = 0.55$ s) by high pressure from the front of the valve, and flow is straight along with the valve. When the flow rate reached the maximum value, the valve is maximum opened. The vortices appear on the backside of the valve when the valve is opened. In the diastole phase, flow is reversed, and the valve is closed ($t = 2.2$ s). In this period, the pressure is negative, and many vortices of fluid flow in the valve.

Figure 9 shows the vorticity corresponding to the instant time in Fig. 8. In all cases, the vorticity reached a big value at the interface of the valve where the direction of blood is changed. This vorticity affects the shear force of the valve into the blood and may be a cause related to blood clotting problems. The results can be used to predict the TAVI for treating cardiovascular disease patients.

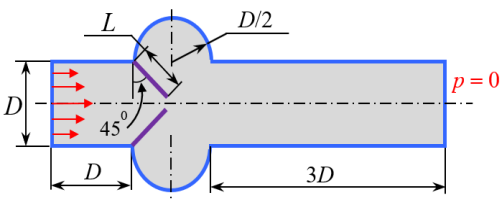


*Fig. 6. Schematic of the flow in a 2D heart valve.*

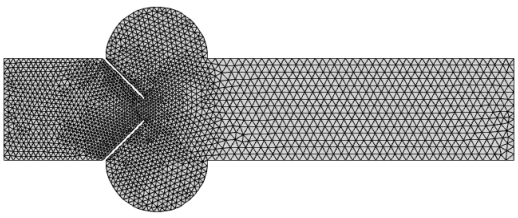

*Fig. 7. Grid for fluid domain.*

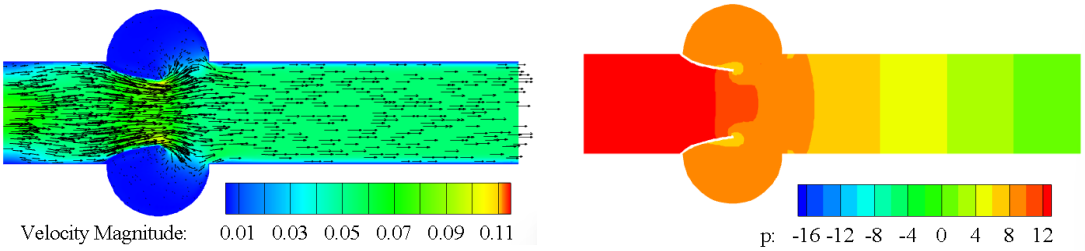


*a) Time = 0.55 s*

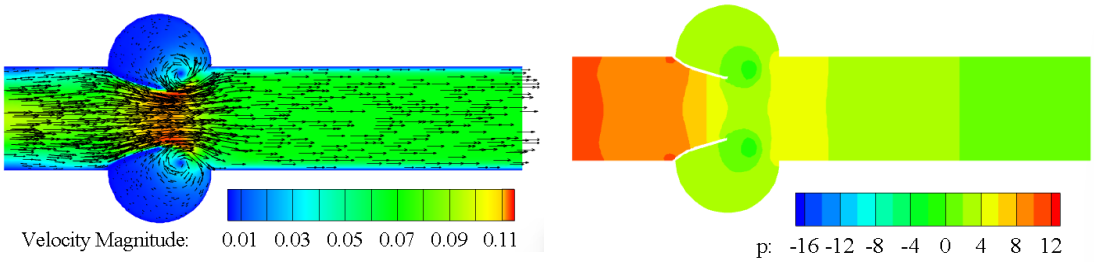


*b) Time = 0.82 s*

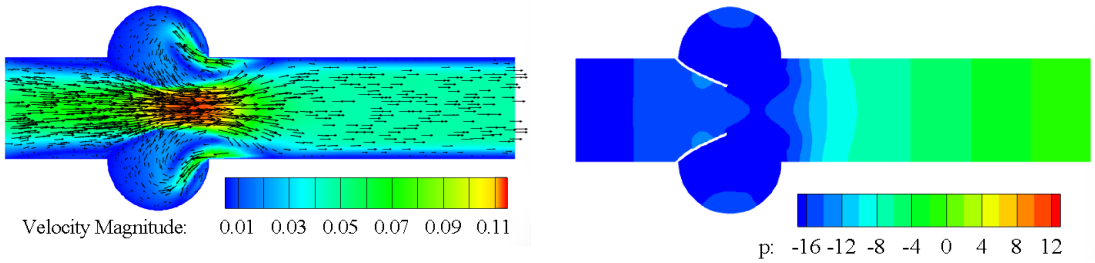


*c) Time = 1.6 s*

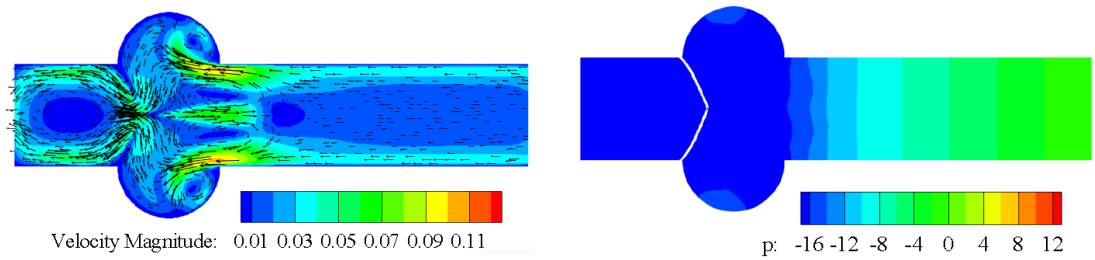


*d) Time = 2.2 s*

*Fig. 8. Velocity field (left) and pressure contour (right) of flow through aortic valve in difference instant time.*

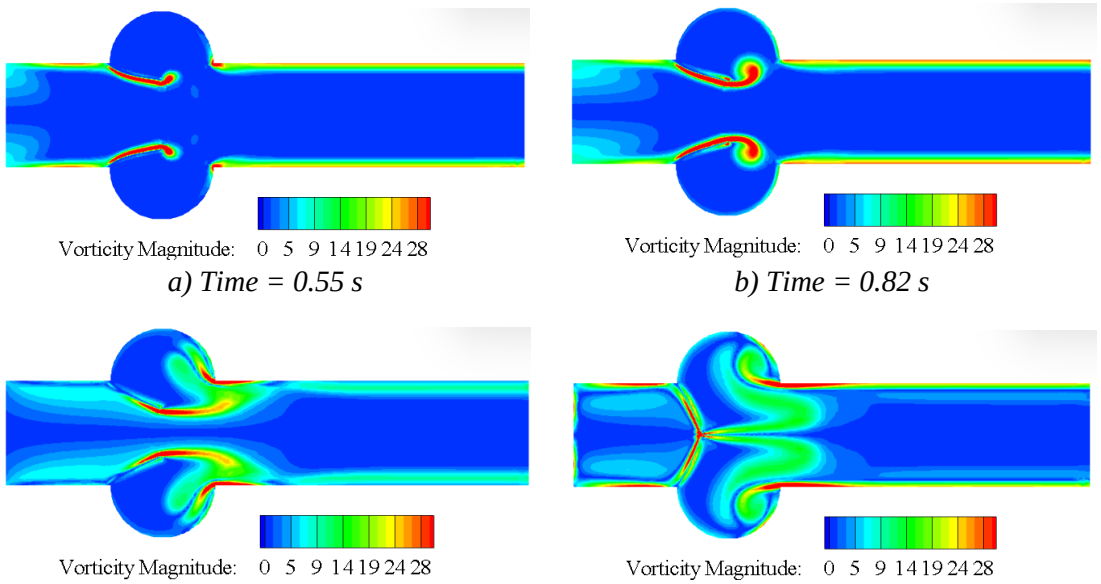


*a) Time = 0.55 s* *b) Time = 0.82 s*

*c) Time = 1.6 s* *d) Time = 2.2 s*

*Fig. 9. Vorticity of flow through aortic valve in difference instant time.*

### *3.3. 3D problem*

Lastly, a 3D problem of blood flow interacting with three leaflets of an aortic valve is simulated. The geometry is shown in Fig. 10, and the dimension is set similarly to those in [12]. A time-dependent velocity, as shown in Fig. 11, is set at the inlet while a zero pressure is set at the outlet for all simulation time. This flow rate is from the left ventricle with the systolic phase (opened valve) and the diastole phase (closed valve) in a period of T = 1.0 s. Fig. 12 shows the streamline and velocity field when the valve is at maximum opening. In addition to the results of the 2D case in section 3.2, the 3D effect is appeared by many vortices after the valve since the geometry is not completely symmetrical. The deformation of the valve is large, and its movement in several instants time is illustrated in Fig. 13. This movement is helpful for the prediction of the TAVI in the real case.

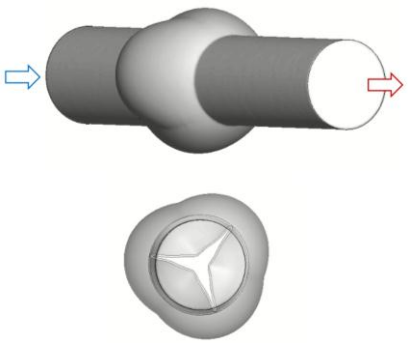

*Fig. 10. Geometry of a 3D aortic valve.*

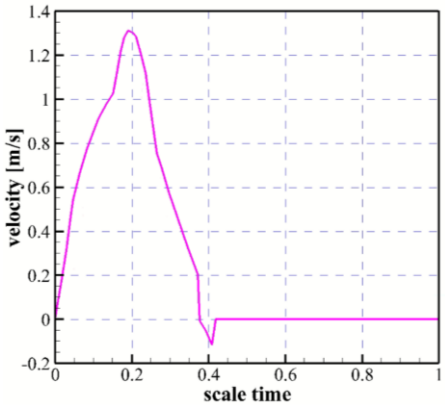


*Fig. 11. Boundary condition on inlet [13].*

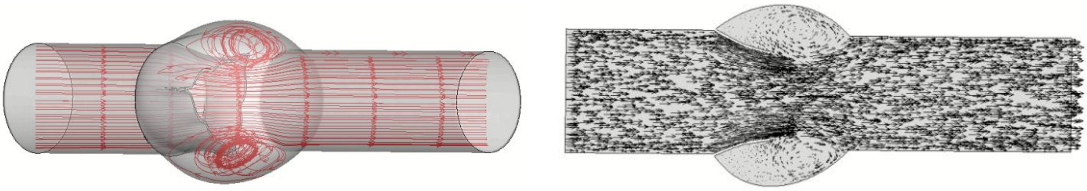

*a) Streamline* *b) Velocity field*

*Fig. 12. Blood flow through the valve at opening phase.*

*a) 0.05T* *b) 0.2T* *c) 0.8T*

*Fig. 13. Deformation of valve at different phases.*

## 4. Conclusion

The study employed the finite element method to discrete the fluid and solid domains for the FSI problem of a complex geometry aortic valve in 2D/3D space. The strong coupling approach with smoothing technique is used to improve the mesh quality of a fluid region. The large deformation model is adopted for elastic solid. The program is validated by simulating a fluid flow in a circle channel, and then it is applied to simulate the blood flow interacting with an aortic valve in 2D and 3D cases. A pulsatile flow at the inlet moves the valve according to the systolic and diastole phase. The results show that the code can simulate the FSI problem with an efficient performance. The simulation results can be used to predict the movement of the valve in the aorta and, therefore, can be helpful in biomechanical problems, especially for the TAVI, such as the prediction of blood clotting problems in the valve.

## References

[1] B. Su, L. Zhong, X. K. Wang, J.M. Zhang, R.S. Tan, J.C. Allen, S.K. Tan, S. Kim, H.L. Leo, "Numerical simulation of patient-specific left ventricular model with both mitral and aortic valves by FSI approach", *Computer methods and programs in biomedicine*, 113(2), pp. 474-482, 2014. doi.org/10.1016/j.cmpb.2013.11.009

[2] A. Amindari, L. Saltik, K. Kirkkopru, M. Yacoub, H.C. Yalcin, "Assessment of calcified aortic valve leaflet deformations and blood flow dynamics using fluid-structure interaction modeling", *Informatics in Medicine Unlocked*, 9, pp. 191-199, 2017. doi.org/10.1016/j.imu.2017.09.001

[3] A.M. Bavo, G. Rocatello, F. Iannaccone, J. Degroote, J. Vierendeels, and P. Segers, "Fluid-structure interaction simulation of prosthetic aortic valves: comparison between immersed boundary and arbitrary Lagrangian-Eulerian techniques for the mesh representation", *PLoS One*, 11(4), e0154517, 2016. doi.org/10.1371/journal.pone.0154517

[4] G. Marom, R. Haj-Ali, E. Raanani, H. J. Schäfers, and M. Rosenfeld, "A fluid-structure interaction model of the aortic valve with coaptation and compliant aortic root", *Medical & Biological Engineering & Computing*, 50(2), pp. 173-182, 2012. DOI: 10.1007/s11517-011-0849-5

[5] K. Dumont, J.M.A. Stijnen, J. Vierendeels, F.N. van de Vosse, and P.R. Verdonck, "Validation of a Fluid-Structure Interaction Model of a Heart Valve using the Dynamic Mesh Method in Fluent", *Computer Methods in Biomechanics and Biomedical Engineering*, 7(3), pp. 139-146, 2004. doi.org/10.1080/10255840410001715222

[6] S.T. Ha, H.G. Choi, *Simulation of the motion of a carotid artery interacting with blood flow by using a partitioned semi-implicit algorithm*, Korean Soc. Comput. Fluids Eng., 2019.

[7] T.S. Ha, V.C. Vu, M.H. Nguyen, and M. D. Nguyen, "Numerical simulation for fluid-structure interaction of a blood flow with the aortic valve using the FEM monolithic formulation", *Journal of Science and Technique*, 16(03), pp. 49-60, 2021. doi.org/10.56651/lqdtu.jst.v16.n03.277

[8] G.A. Holzapfel, "Nonlinear solid mechanics: A continuum approach for engineering Science", *Meccanica*, 37(4/5), pp. 489-490, 2002.

[9] S.T. Ha, H.G. Choi, "Investigation on the effect of density ratio on the convergence behavior of partitioned method for fluid-structure interaction simulation", *Journal of Fluids and Structures*, 96, p. 103050, 2020. doi.org/10.1016/j.jfluidstructs.2020.103050

[10] S.T. Ha, H.G. Choi, "A meshless geometric multigrid method based on a node-coarsening algorithm for the linear finite element discretization," *Computers & Mathematics with Applications*, 96, pp. 31-43, 2021. doi.org/10.1016/j.camwa.2021.05.009

[11] H.G. Kim, "A new coupling strategy for fluid-solid interaction problems by using the interface element method", *Int. J. Numer. Meth. Eng.*, 81, pp. 403-428, 2010. doi.org/10.1002/nme.2698

[12] S.T. Ha, T.D. Nguyen, V.C. Vu, M.H. Nguyen, M.D. Nguyen, *A Study of Fluid-Structure Interaction of Unsteady Flow in the Blood Vessel Using Finite Element Method*, In Modern Mechanics and Applications, 2022, pp. 1089-1101, Springer, Singapore. doi.org/10.1007/978-981-16-3239-6_85

[13] H.S. Jeannette, J. Johan, J. Niclas, H. Johan, "3D Fluid-Structure Interaction Simulation of Aortic Valves Using a Unified Continuum ALE FEM Model," *Frontiers in Physiology*, 9, p. 363, 2018. doi.org/10.3389/fphys.2018.00363

# PHƯƠNG PHÁP SỐ NGHIÊN CỨU DÒNG MÁU CHUYỂN ĐỘNG QUA VAN ĐỘNG MẠCH CHỦ

**Hà Trường Sang, Nguyễn Trung Định, Vũ Văn Chiên, Nguyễn Mạnh Hùng, Vũ Đức Quyến, Nguyễn Mạnh Đức**

***Tóm tắt:*** *Bài báo trình bày việc phân tích tính toán dòng máu chuyển động qua van động mạch chủ sử dụng mô phỏng tương tác chất lỏng và cấu trúc. Phương pháp phần tử hữu hạn được sử dụng cho cả miền chất lỏng và cấu trúc, và mô hình đơn khối được dùng cho sự kết hợp của pha cấu trúc và lỏng để giải quyết tốt hai thử thách đó là hiệu ứng cộng khối và vấn đề biến dạng lớn của tường vật rắn. Phương pháp tích phân dựa trên lưới di động không cấu trúc Euler-Lagrange được áp dụng để giải hệ phương trình Navier-Stokes cho dòng chất lỏng không nén được và công thức tổng hợp Lagrange được dùng cho trạng thái phi tuyến của van. Kỹ thuật làm mịn lưới dựa trên phương trình Laplace được ứng dụng để nâng cao chất lượng lưới của vùng chất lỏng trong cả không gian 2 và 3 chiều. Các đại lượng đặc trưng cho dòng chảy như vận tốc và áp suất được đánh giá và phân tích cụ thể. Kết quả mô phỏng cho thấy vận tốc và áp suất đạt giá trị lớn nhất tại thời điểm van mở lớn nhất. Mặt khác, có thêm nhiều xoáy xuất hiện phía sau van trong giai đoạn đóng. Kết quả mô phỏng có thể giúp ích cho việc chẩn đoán và điều trị các bệnh hệ tim mạch.*

**Từ khóa:** Dòng mạch máu; van tim; tương tác chất lỏng-cấu trúc; FEM; ALE.

*Received:* 29/11/2021; *Revised:* 13/10/2022; *Accepted for publication:* 11/11/2022

❑